JOURNAL OF SOLID STATE CHEMISTRY 58, 187–193 (1985)

Thermal Decomposition of Chromium Oxide Hydroxide

I. Effect of Particle Size and Atmosphere

SHIGEHARU KITTAKA, TOHRU MOROOKA, AND KOHJI KITAYAMA

Department of Chemistry, Okayama College of Science, 1-1 Ridaicho, Okayama 700, Japan

AND TETSUO MORIMOTO

Department of Chemistry, Faculty of Science, Okayama University, Tsushima, Okayama 700, Japan

Received January 24, 1984; in final form November 19, 1984

The thermal decomposition process of α-$HCrO_2$ and β-$HCrO_2$ having various crystal habits and sizes was studied in an atmosphere of H_2O, O_2, and air by means of thermal gravimetry, high temperature X-ray diffraction analysis, and electrical conductivity measurement. In H_2O vapor both α-$HCrO_2$ and β-$HCrO_2$ were decomposed directly into crystalline Cr_2O_3 through the reaction $2HCrO_2 \rightarrow Cr_2O_3 + H_2O$. In the presence of O_2, however, the decomposition temperature was lower than that in H_2O vapor and a two-stepped thermal decomposition spectrum (two peaks) was obtained. Two steps were clearly separated on the β-$HCrO_2$ and assigned, respectively, to the reactions $2HCrO_2 + \frac{1}{2}O_2 \rightarrow 2CrO_2 + H_2O$ and $2CrO_2 \rightarrow Cr_2O_3 + \frac{1}{2}O_2$. On the α-$HCrO_2$ samples the first reaction was newly found and followed by the second reaction at higher temperatures. The atoms in the crystal of α-$HCrO_2$ and β-$HCrO_2$ were found to start internal migration at about 200 and 250°C, respectively.

Introduction

The thermal decomposition of metal hydroxides and hydrous metal oxides are important research subjects in the fields of catalysis and surface chemistry (*1, 2*). In this process many such complicated steps as scission–recombination of chemical bonds, atomic diffusion, micropore formation, recrystallization, sintering, etc., are involved. Moreover, oxidation or reduction processes of metal ions may also be concerned depending on the atmosphere. Among the works on chromium compounds carried out from such viewpoints, hydrous Cr_2O_3 is the most widely investigated material (*1–4*) because of the high activity of the decomposition product, Cr_2O_3, as an oxidation or reduction catalyst. With $HCrO_2$-type hydroxides, however, less work has been reported. The decomposition of β-$HCrO_2$ has been carefully examined under various conditions by Alario Franco *et al.* (*5–8*) and it was reported that β-$HCrO_2$ could be decomposed into Cr_2O_3 through ferromagnetic CrO_2 as a transition product even in a vacuum. On the other hand, work on α-$HCrO_2$ has not reported the thermal

0022-4596/85 $3.00

decomposition, but only the characteristic position of H atoms, which are situated between layers to form H bonds, as determined by IR spectroscopy, neutron diffraction, and NMR (*9–11*).

The present authors have found that the surfaces of α-$HCrO_2$ and its thermal decomposition product Cr_2O_3 have marked homogeneity for the adsorption of H_2O and Kr gases, where stepwise adsorption isotherms have been found (*12*). As the decomposition mechanisms, however, have not been elucidated, the present paper will be concerned with the decomposition process of α-$HCrO_2$ in the atmosphere of O_2, air, and H_2O in comparison with that of β-$HCrO_2$.

Experimental

Materials

The α-$HCrO_2$ samples (A-1 to A-4) tested here were formed by hydrolysis of $Cr(NO_3)_3$ according to the reaction

$$Cr(NO_3)_3 + 2H_2O \rightarrow HCrO_2 + 3HNO_3. \quad (1)$$

in an autoclave under various conditions shown in Table I. NO_2 gas was detected after preparation but the oxidation of Cr^{3+} to a higher oxidation state was not observed. Sample A-5 was prepared by hydrothermal treatment of hydrous Cr_2O_3 precipitated from $Cr(NO_3)_3$ solution with NH_3 solution. β-$HCrO_2$ (B-1) was formed through stepwise reductions (*8, 13*): (1) decomposition of CrO_3 into CrO_2 under high O_2 pressure in an autoclave; (2) hydrogenation of CrO_2 in H_2 to β-$HCrO_2$. All the samples prepared were purified by electrodialysis and dried at 110°C in an electric oven. The crystal structure was confirmed by powder X-ray diffraction using Cu*K*α and the particle shapes by electron microscopy (SEM and TEM). Figure 1 shows that the α-$HCrO_2$ samples formed at lower temperatures and lower concentrations of $Cr(NO_3)_3$ have the shape of a hexagonal single crystal platelet as expected from the crystal structure $R\bar{3}m$. With an increase in reaction temperature and/or concentration larger and thicker particles were obtained. According to more detailed examinations, growth along the *c* axis was more marked than that along the *a* and *b* directions. The β-$HCrO_2$ obtained were polyhedral particles.

TABLE I

PREPARATION CONDITIONS OF α-$HCrO_2$ AND β-$HCrO_2$

Sample	Conditions	D_{003}[a] (Å)	S[b] ($m^2 \cdot g^{-1}$)
α-$HCrO_2$			
A-1	0.3 *M* $Cr(NO_3)_3$, 200°C, 2.5 MPa, 1 hr	190	48.0
A-2	0.3 *M* $Cr(NO_3)_3$, 300°C, 30 MPa, 1 hr	500	15.2
A-3	0.1 *M* $Cr(NO_3)_3$, 300°C, 30 MPa, 1 hr	460	20.1
A-4	1.0 *M* $Cr(NO_3)_3$, 300°C, 30 MPa, 1 hr	1600	9.19
A-5	$Cr_2O_3 \cdot nH_2O$, 400°C, 150 MPa, 24 hr	2500	4.14
β-$HCrO_2$			
B-1	CrO_3, O_2 17.0 MPa, 350°C, 4 hr CrO_2, H_2 10 kPa, 330°C, 30 hr	—	6.99

[a] Thickness of the particles along the *c* axis determined by the line broadening of the 003 X-ray diffraction peak.

[b] Specific surface area.

Thermal Decomposition Spectra and Electrical Conductivity

The thermal decomposition spectra were measured with the Sartorius vacuum microbalance attached to gas-controlling and temperature-controlling systems made by Chino Company (*14*). Decomposition was carried out under the gaseous condition: H_2O vapor of 610 Pa was controlled by keeping the temperature of the trap at 0°C, O_2 was supplied at the rate of 50 ml $\cdot$ min^{-1} from an O_2 cylinder, and air was leaked by opening the gas-controlling system to air. The standard heating rate was $\frac{5}{6}$°C $\cdot$ min^{-1}.

The electric conductivity of the sample was measured by using a DC method, in

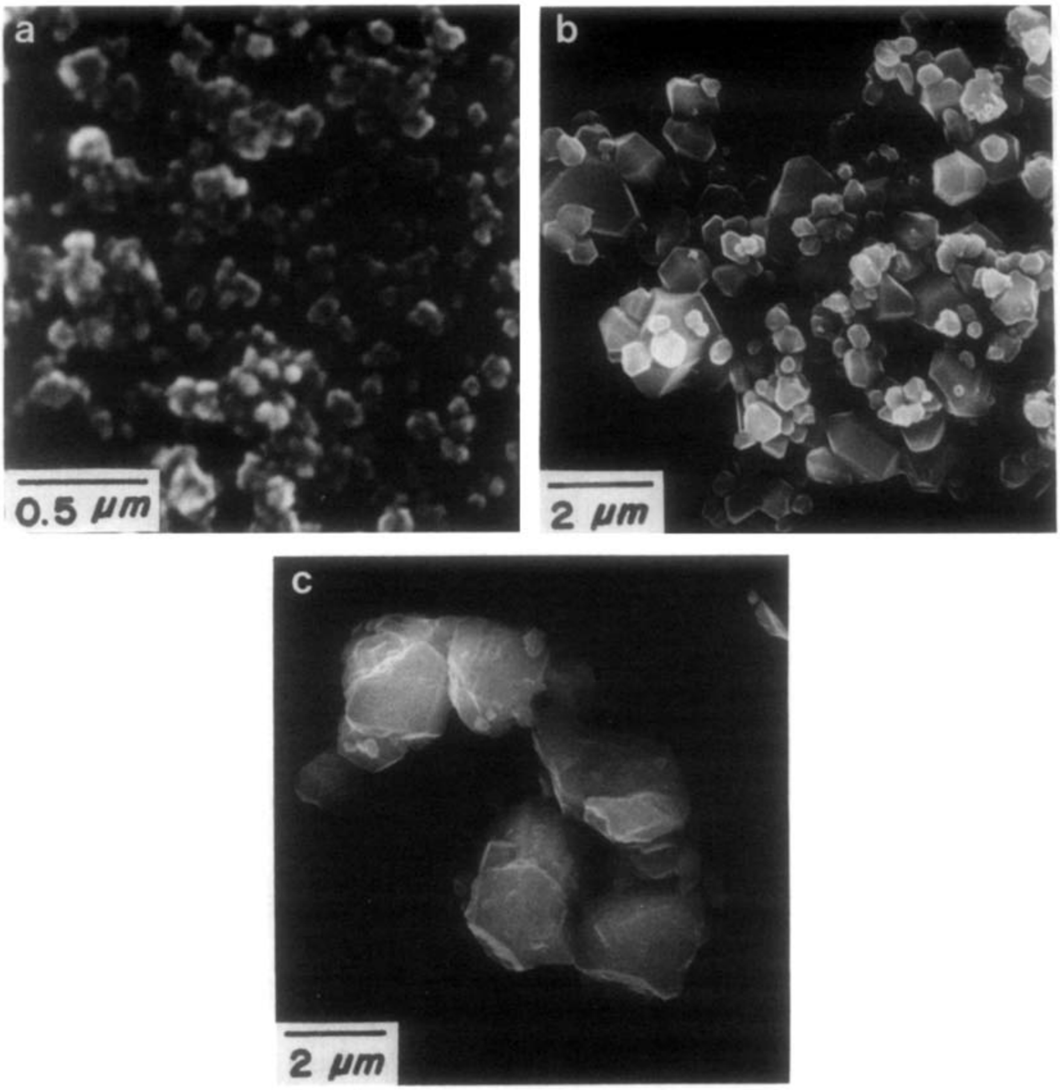

FIG. 1. Scanning electron micrographs of α-$HCrO_2$ A-1 (a) and A-5 (b) and β-$HCrO_2$ B-1 (c).

which the sample slurry was spread between a couple of 400°C-evacuated Ag electrodes separated by 5 mm on the silica glass plate. The electric potential applied to the electrodes was 1.5 V from six dry cells connected in parallel.

Thermal Decomposition Rate

The thermal decomposition rate was measured by use of the TGD-5000 (ULVAC SINKU-RIKO) equipped with an infrared image furnace by which the temperature of the sample could be raised from 50 to 430°C within 20 sec. This rapid heating caused a little vibration of the sample which stopped a few seconds after attainment of the expected temperature of 430°C. The reproducibility of the experiments was not satisfactory for the analysis of the decomposition kinetics probably due to the difference of sampling conditions.

Results and Discussion

Thermal Decomposition in H_2O

Figures 2a–c show the thermal decomposition spectra for α-$HCrO_2$ (A-3 and A-5) and β-$HCrO_2$ (B-1) determined in O_2, air, and H_2O. When the samples were heated in H_2O vapor, a single peak was observed in the narrow range of 480–490°C, as can be seen in Fig. 2. According to the high temperature X-ray analysis these samples were decomposed directly into crystalline Cr_2O_3 without going through the amorphous Cr_2O_3, observed in the decomposition of hydrous Cr_2O_3 (2):

$$2HCrO_2 \rightarrow Cr_2O_3 + H_2O. \quad (2)$$

Figure 2b shows that the increase in vapor pressure of H_2O gives rise to the increase in the decomposition temperature and rationally the decomposition *in vacuo* occurs at a temperature lower than that in H_2O vapor. This kind of phenomenon can be expected from reaction (2) and has been reported on $Mg(OH)_2$ by Freund (*15*). The decomposition temperature was found to increase by about 20°C from A-1 through A-5 at 610 Pa of H_2O.

Figure 3 shows the effect of preheating on the decomposition rates of α-$HCrO_2$

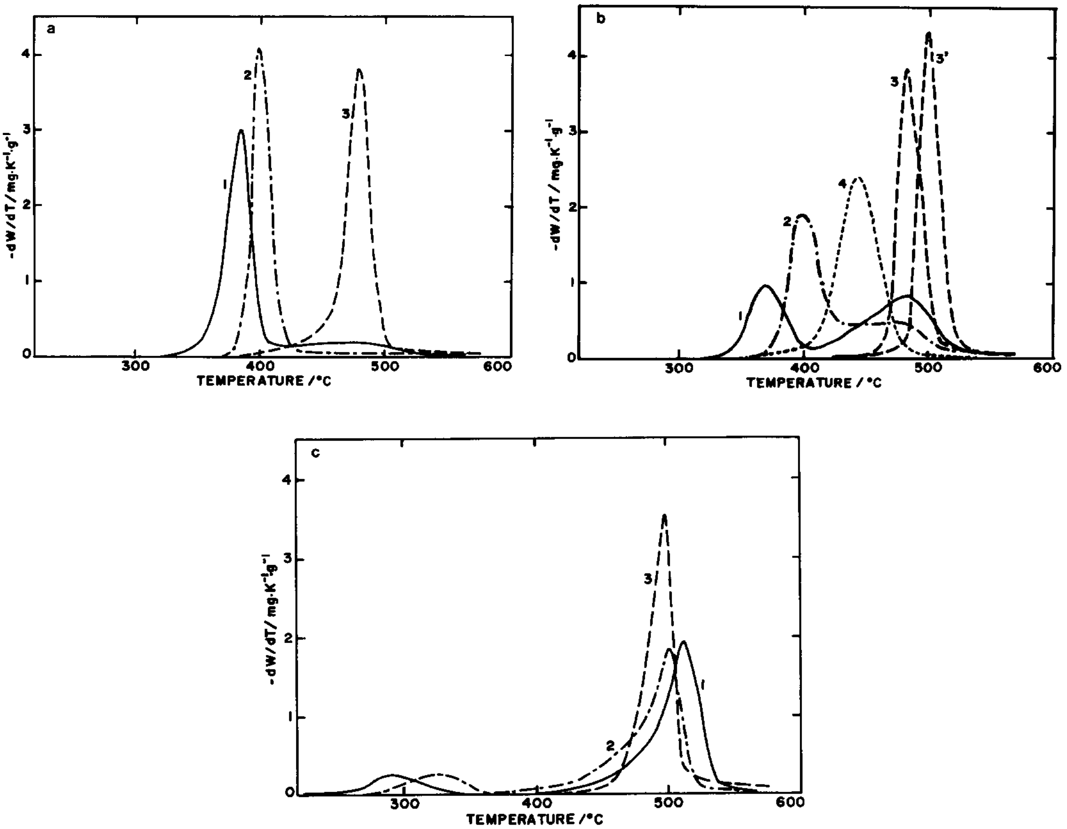

FIG. 2. (a) Thermal decomposition spectra of α-$HCrO_2$ A-3. Atmosphere: (1) O_2; (2) air; (3) H_2O. Heating rate: $\frac{5}{6}$°C · min^{-1}; (b) Thermal decomposition spectra of α-$HCrO_2$ A-5. Atmosphere: (1) O_2; (2) air; (3) H_2O vapor at 0°C; (3′) H_2O vapor at 28.0°C; (4) vacuum. Heating rate: $\frac{5}{6}$°C · min^{-1}; (c) Thermal decomposition spectra of β-$HCrO_2$ (B-1). Atmosphere: (1) O_2; (2) air; (3) H_2O. Heating rate: $\frac{5}{6}$°C · min^{-1}.

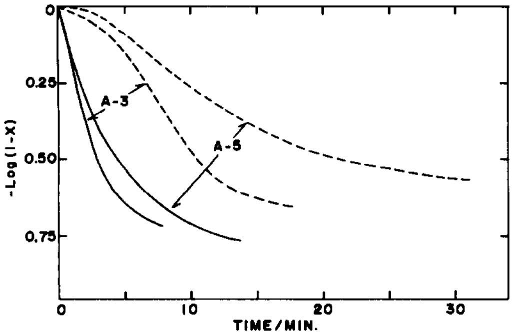

FIG. 3. Weight loss of α-$HCrO_2$ A-3 and A-5 in H_2O at 430°C as a function of time. Original sample—solid line; pretreated at 300°C in H_2O vapor for 90 min—broken line. x—the ratio of the removed H_2O to the component H_2O of the sample.

(A-3 and A-5) in H_2O vapor. When untreated samples are heated in a short time from 50 to 430°C, which is lower than the temperature of decomposition in Figs. 2a and b, and kept at constant temperature, they are decomposed quite rapidly. If these samples are preheated in H_2O vapor for 90 min at 300°C, the decomposition rate is markedly depressed. Moreover, the 300°C-preheated sample gave a decomposition temperature slightly lower but very similar to that of the untreated sample, which suggests that the slow heating rate of $\frac{5}{6}\,^{\circ}\mathrm{C} \cdot \mathrm{min}^{-1}$ should work as the aging effect before the decomposition starts. The electron microscopic observation and X-ray diffraction analysis did not show any changes in the crystalline size before and after the heat treatment at 300°C. So it can be suggested that some lattice defects of the crystalline samples which might be produced during preparation were relieved by preheating to give more perfect crystals.

Thermal Decomposition in O_2

The presence of O_2 decreased the starting temperature of decomposition significantly from that in the presence of H_2O: the higher the O_2 pressure the lower the decomposition temperature (Figs. 2a–c). At the same time a shoulder or another peak appeared, which had never been observed with α-$HCrO_2$. Especially with β-$HCrO_2$ two peaks appeared at 290 and 505°C in O_2, and at 320 and 500°C in air. The ratio of the low-temperature peak area to the high-temperature peak area was 1 : 8, which indicates that each peak originates, respectively, from the reactions

$$2HCrO_2 + \tfrac{1}{2}O_2 \rightarrow 2CrO_2 + H_2O \quad (3)$$

$$2CrO_2 \rightarrow Cr_2O_3 + \tfrac{1}{2}O_2. \quad (4)$$

High-temperature X-ray diffraction analysis substantiated the formation of the reaction products CrO_2 and Cr_2O_3 at each temperature range correspondingly to reactions (3) and (4). In the case of α-$HCrO_2$, however, it is suggested that the high-temperature peak can be assigned to reaction (4), but the low-temperature peak is composed of reactions (2) and (3), which are confirmed by the simultaneous presence of $HCrO_2$, CrO_2, and Cr_2O_3, as shown in the X-ray analysis of Fig. 4a. Of course the ratios between them vary with samples: in the largest particles of A-5 the main components were $HCrO_2$ and CrO_2 (Fig. 4b).

Figure 5 shows the thermal decomposition spectra of α-$HCrO_2$ (A-1–A-5) in O_2. The samples of thin plates (A-1 and A-3) gave a large low-temperature peak and a small high-temperature peak, while the increase in the thickness (A-4 and A-5) leads to enhancement of the latter. According to the electron diffraction analysis the sample of A-3 heated at 600°C gave a hexagonally symmetrical diffraction pattern for the single crystal particle of Cr_2O_3, which suggests the occurrence of the topotactic decomposition of hexagonal α-$HCrO_2$ to Cr_2O_3 of the same crystal type. Particles of thick samples, A-4 and A-5, were collapsed. This would be due to the stepwise changes of different crystal structure in O_2 from hexagonal (α-$HCrO_2$) via tetragonal (CrO_2) to

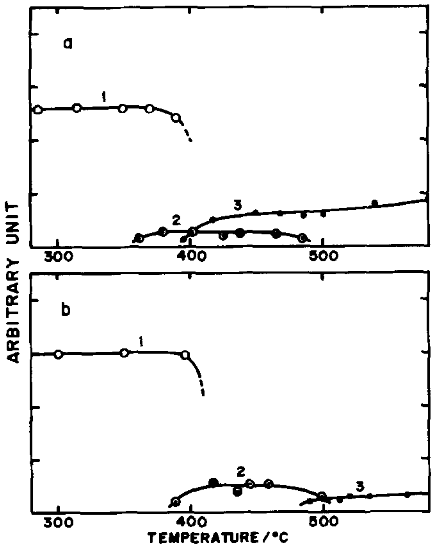

FIG. 4. Peak heights of X-ray diffraction of α-$HCrO_2$ heated in O_2 at increasing temperatures: (a) A-3; (b) A-5. Diffraction indices: (1) 003 α-$HCrO_2$; (2) 110 CrO_2; (3) 104 Cr_2O_3. Heating rate: $\frac{5}{6}$°C · min^{-1}.

hexagonal (Cr_2O_3) form and density changes.

Several works have reported that orthorhombic β-$HCrO_2$ can easily be oxidized into tetragonal CrO_2 which has been tested for ferromagnetic material (*8, 16, 17*). The ease of this reaction has been attributed to the very similar relative positions of Cr and O in β-$HCrO_2$ and CrO_2 (*18, 19*). Thus, it may be possible that the temperature for liberating H^+ ions from the structure is the same temperature for the reaction releasing H^+ from the solid (*3*). Here, the liberation of H^+ was examined through electrical conductivity measurements under H_2O and O_2 vapor as had been applied on $Al(OH)_3$, $Ca(OH)_2$, and $Mg(OH)_2$ under an H_2/N_2 atmosphere by Freund *et al.* (*20*). In the O_2 atmosphere an oxidation reaction occurs on the surface to form higher valent chromium oxides having high electrical conductivity, so that the electrical conductivity increases at a temperature lower than that at which the bulk conductivity increase would start (Fig. 6). Rationally this effect should be marked on the sample with larger specific surface area (S-3) compared to those with smaller areas (S-5 and B-1).

The electrical conductivity of β-$HCrO_2$ in H_2O vapor gave a small peak around 300°C which coincided very well with the low-temperature peak of thermal decomposition curve 1 in Fig. 2c, where the CrO_2 was formed from α-$HCrO_2$ by the reaction of H with O_2 in the atmosphere. Accordingly, this result tells us that the change of electrical conductivity in H_2O is due to the ionic conduction from liberated H^+, which can

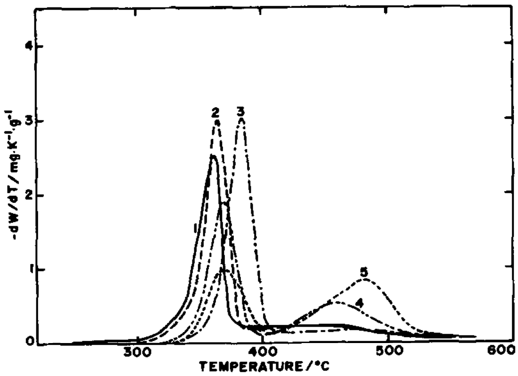

FIG. 5. Thermal decomposition spectra of α-$HCrO_2$ in O_2: (1) A-1; (2) A-2; (3) A-3; (4) A-4; (5) A-5. Heating rate: $\frac{5}{6}$°C · min^{-1}.

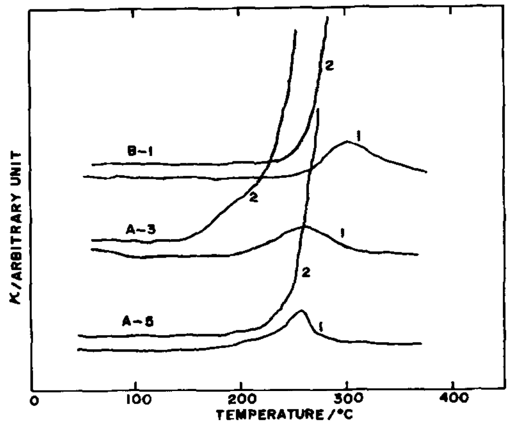

FIG. 6. Electric conductivity (κ) of α-$HCrO_2$ A-3 and A-5 and β-$HCrO_2$ B-1 in H_2O (1) and O_2 (2). Heating rate: $\frac{5}{6}$°C · min^{-1}.

trigger the oxidation reaction (3). In contrast to the result of Alario Franco *et al.* (*6*), weight change by reaction (*5*) was not observed around 300°C (Fig. 2c, curve 1):

$$2HCrO_2 \rightarrow 2CrO_2 + H_2. \qquad (5)$$

In the case of α-$HCrO_2$, the maximum electrical conductivity for samples A-3 and A-5 in H_2O vapor is situated at a temperature around 260°C, 40°C lower than that for β-$HCrO_2$. The oxidation reaction of these samples in O_2, however, starts around 320°C, which is fairly higher than the starting temperature of decomposition for β-$HCrO_2$ (Figs. 2a–c). This difficulty in the oxidation reaction of α-$HCrO_2$ (3) may be explained by the presence of the reconstruction process of the crystal skeleton of Cr^{3+} and O^{2+} from a hexagonal to a tetragonal arrangement, accompanying the liberation of H from the solid. The size effect in Fig. 5 would also be correlated to the process shown above. Once H atoms are removed from the solid in O_2, O^{2-} ions liberated from the α-$HCrO_2$ skeleton may have some energy to migrate into the particle and to be emitted as O_2 through the surface: the smaller particles having larger specific surface area would lose O atoms more efficiently, and immediately after removal of H atoms, would give the product Cr_2O_3, while the thicker particles would leave as CrO_2.

References

1. A. R. Burwell, Jr., G. L. Haller, K. C. Taylor, and J. F. Read, *Adv. Catal.* **20,** 1 (1969).
2. A. Zecchina, S. Coluccia, E. Guglielminotti, and G. Giotti, *J. Phys. Chem.* **75,** 2774 (1971).
3. R. B. Fahim, M. I. Zaki, and N. H. Yacoub, *J. Colloid Interface Sci.* **88,** 502 (1982).
4. A. C. Zettlemoyer, M. Siddiq, and F. J. Micale, *J. Colloid Interface Sci.* **66,** 173 (1978).
5. M. A. Alario Franco and K. S. W. Sing, *An. Quim.* **70,** 41 (1974).
6. M. A. Alario Franco and K. S. W. Sing, *An. Quim.* **71,** 296 (1975).
7. R. S. Puche and M. A. Alario Franco, *An. Quim.* **76,** 213 (1980).
8. M. A. Alario Franco and K. S. W. Sing, *J. Therm. Anal.* **4,** 47 (1972).
9. A. N. Christensen, P. Hansen, and M. S. Lehman, *J. Solid State Chem.* **21,** 325 (1977).
10. R. D. Snyder and J. A. Ibers, *J. Chem. Phys.* **36,** 1356 (1962).
11. M. C. Lawrence and G. N. Robertson, *Mol. Phys.* **43,** 193 (1981).
12. S. Kittaka, R. Fujinaga, K. Morishige, and T. Morimoto, *J. Colloid Interface Sci.* **103,** 453 (1984).
13. F. Kanamaru, private communication.
14. K. Morishige, S. Kittaka, A. Moriyasu, and T. Morimoto, *J. Chem. Soc. Faraday Trans. 1* **76,** 738 (1980).
15. P. D. Garn and F. Freund, *Trans. J. Brit. Ceram. Soc.* **74,** 23 (1975).
16. N. C. Tombs, W. J. Croft, J. R. Carter, and J. J. Fitzgerald, *Inorg. Chem.* **3,** 1701 (1964).
17. K. Yabuta, N. Minomura, M. Shimada, F. Kanamaru, and M. Koizumi, *Mater. Res. Bull.* **13,** 1335 (1978).
18. Y. Shibasaki, F. Kanamaru, and M. Koizumi, *Mater. Res. Bull.* **8,** 559 (1973).
19. M. A. Alario Franco, J. Fenerty, and K. S. W. Sing, "Reactivity of Solids" (J. S. Anderson *et al.*, Eds.), p. 327, Chapman & Hall, London, (1972).
20. F. Freund and H. Wengeler, *Ber. Bunsenges. Phys. Chem.* **84,** 866 (1980).